Available online at www.sciencedirect.com

SciVerse ScienceDirect

Ceramics International 39 (2013) 1503–1510

CERAMICS INTERNATIONAL

www.elsevier.com/locate/ceramint

Antibacterial and photocatalytic properties of $Ag/TiO_2/ZnO$ nano-flowers prepared by facile one-pot hydrothermal process

Hem Raj Pant[a,b,*], Bishweshwar Pant[a], Ram Kumar Sharma[b], Altangerel Amarjargal[a,c], Han Joo Kim[d], Chan Hee Park[a], Leonard D. Tijing[d], Cheol Sang Kim[a,d,*]

[a]Department of Bio-nano System Engineering, Chonbuk National University, Jeonju 561-756, Republic of Korea
[b]Department of Engineering Science and Humanities, Institute of Engineering, Pulchowk Campus, Tribhuvan University, Kathmandu, Nepal
[c]Power Engineering School, Mongolian University of Science and Technology, Ulaanbaatar, Mongolia
[d]Division of Mechanical Design Engineering, Chonbuk National University, Jeonju 561-756, Republic of Korea

Received 2 July 2012; received in revised form 26 July 2012; accepted 29 July 2012
Available online 8 August 2012

Abstract

In this paper, a simple and efficient strategy of one-pot synthesis of Ag doped TiO_2/ZnO photocatalyst was developed using hydrothermal process. Simultaneous crystallization of Ag and ZnO crystals from their precursor solution containing P25 (TiO_2) NPs could form effectively bonded $Ag/TiO_2/ZnO$ composite photocatalyst during hydrothermal treatment. Several analytical techniques, including scanning electron microscopy (SEM), transmission electron microscopy (TEM), X-ray diffraction (XRD), FT-IR spectroscopy, and photoluminescence spectroscopy have been used to characterize the resulting $Ag/TiO_2/ZnO$ photocatalyst. Results showed that ZnO nano-flowers doped with TiO_2 and Ag NPs were formed by this simple facile one-step process. The unique properties of Ag NPs on binary semiconductor composite not only provide the decreased rate of electron–hole separation but also prevent from the loss of photocatalyst during recovery due to the fixed attachment of Ag and TiO_2 NPs on the surface of flower shaped large ZnO particles. Therefore, as-synthesized composite is an economically and environmentally friendly photocatalyst.

Keywords: B. Composite; Hydrothermal; Photocatalyst; Ag NPs

1. Introduction

Semiconductor materials such as TiO_2 and ZnO micro/nano-particles are the most promising materials for remediation and destruction of organic pollutants under UV-irradiation [1]. Both metal oxides exhibit very similar band gaps (ZnO, 3.37 eV and TiO_2, 3.2 eV) and their physicochemical properties are tunable by controlling the structure and surface area of the particles [2–4]. Different development has been carried out to increase the surface area of these photocatalytic particles [5,6]. Decreasing particle size is one effective way to increase the surface area of photocatalyst. However, the agglomeration of such extremely nano-sized particles and difficulty of their recovery from the reaction system after photocatalysis hinders their application in this field [7–9]. Furthermore, the photoexcited electrons and holes (e–h) can also recombine to reduce photocatalytic activity of pristine semiconductors particles. Our previous report shows that the photocatalytic property of ZnO particles is increased when TiO_2 NPs are doped on the surface of ZnO flowers [3]. Therefore, the strategy of doping silver (Ag) NPs on the surface of this composite could further enhance the photocatalytic activity by preventing the fast e–h recombination process [10–12]. Moreover, doping of Ag NPs on this binary semiconductor composite particle might possess good antibacterial property even in the absence of UV-light.

Silver doped ZnO or TiO_2 NPs are now an exciting area in research for developing photocatalytic applications [13–15]. Ag is known as electron sinks due to the Schottky

*Corresponding authors at: Department of Bio-nano System Engineering, Chonbuk National University, Jeonju 561-756, Republic of Korea. Tel.: +82 63 270 4284; fax: +82 63 270 2460.
E-mail addresses: hempant@jbnu.ac.kr (H.R. Pant), chskim@jbnu.ac.kr (C.S. Kim).

0272-8842/$ - see front matter © 2012 Elsevier Ltd and Techna Group S.r.l. All rights reserved.
http://dx.doi.org/10.1016/j.ceramint.2012.07.097

barrier at the metal–semiconductor interface [16,17]. Although there are many reports about the effect of Ag NPs on photochemical properties of semiconductors, to the best of our knowledge, there is no report on the fabrication of mixed binary semiconductor nanocomposite decorated with Ag NPs using one-pot synthesis process. In this present work, a simple and effective strategy of simultaneous crystal growth of Ag and ZnO particles from the hydrothermal solution containing P25 (TiO_2) NPs was developed to synthesis $Ag/TiO_2/ZnO$ photocatalyst. As-synthesized photocatalyst not only increases the photodegradation of dyes under UV-radiation but also shows the antibacterial activity even in the absence of UV-light. Furthermore, large ZnO flowers (having extremely small size Ag and TiO_2 NPs) with highly open morphology shows the perfect recovery of catalyst after reaction and its unchanged efficiency for cyclic use shows that it will be an economically and environmentally friendly photocatalyst.

2. Experimental

2.1. Materials

Commercially available TiO_2 NPs (Aeroxide P25, 80% anatase 20% rutile, average particle size of 21 nm and specific surface area $50 \pm 15\ m^2\ g^{-1}$), Zinc nitrate hexahydrate, bis-hexamethylene triamine, silver nitrate, and reactive black 5 (all AR grade reagents) were used without any further purification.

2.2. Preparation of photocatalyst

$Ag/TiO_2/ZnO$ composite particles were synthesized by hydrothermal treatment of aqueous suspension of the mixture of 20 mg TiO_2 in 10 ml ethanol, 10 ml of 5.88×10^{-3} M $AgNO_3$, 40 ml of 0.058 M of bis-hexamethylene triamine, and 40 ml of 0.063 M zinc nitrate hexahydrate. At first, bis-hexamethylene triamine and zinc nitrate hexahydrate solutions were mixed and slurry was made by vigorously stirring for 1 h and then solution of $AgNO_3$ and P25 were added to this solution with further 0.5 h stirring. Similarly, the pristine ZnO was prepared without $AgNO_3$ and TiO_2, and TiO_2/ZnO hybrid nanocomposite was prepared without $AgNO_3$ [3]. The solution was then taken into a Teflon crucible and kept inside the autoclave. In each case, the autoclave with Teflon crucible (containing solution) was kept at 140 °C for 2 h. The obtained product after cooling was filtered off, washed several times by distilled water and alcohol, and dried at 130 °C for 12 h to increase the crystalinity and remove the moisture from the photocatalyst.

2.3. Characterization

The morphology of the as-prepared photocatalysts was observed by using FE-SEM (S-7400, Hitachi, Japan). TEM images and line EDX were observed using transmission electron microscopy (JEM-2200, JEOL, Japan). Information about the phase and crystallinity was obtained with a Rigaku X-ray diffractometer (XRD, Rigaku, Japan) with Cu Kα ($\lambda = 1.540$ Å) radiation over Bragg angles ranging from 10° to 80°. Fourier transform infrared (FT-IR) spectra of different samples were recorded by using an ABB Bomen MB100 Spectrometer (Bomen, Canada). Room temperature photoluminescence (PL) spectrum was recorded by Perkin Elmer Instruments (LS-55).

2.4. Photocatalytic and antibacterial properties

The photocatalytic activity of as-prepared photocatalysts was evaluated by observing the degradation of aqueous solution of reactive black 5. The process was carried out in a 100 ml beaker which was equipped with the tip of a light-guide (5 mm in diameter) of mercury-vapor lamp (Omni-Cure, EXFO). The UV light with intensity of 20% was used in this experiment. The distance between solution and tip of light-guide was 5 cm. In each case, 30 ml dye solution (10 ppm concentration) and 10 mg catalyst were mixed to make suspension by stirring for 30 min in dark to ensure adsorption/desorption equilibrium prior to UV irradiation. At specific time intervals, 1 ml of the sample was withdrawn from the system and centrifuged to separate the residual catalyst, and then the absorbance intensity was measured at the corresponding wavelength using UV–visible spectrophotometer (HP 8453 UV–visible spectroscopy system, Germany). For cycling use experiments, $Ag/TiO_2/ZnO$ NPs were separated from suspended solution by repeated centrifuging and washing process.

Similarly, antibacterial test was carried out using *Escherichia coli* (*E. coli*) suspension under UV radiation of 20% intensity. The working suspensions were prepared by adding 200 μl of inoculated LB medium to a 50 ml sterilized distilled water in a beaker. The antibacterial experiment was carried out in a sterilized 100 ml glass beaker containing *E. coli* suspension (50 ml) and 0.4 g/l of different photocatalysts with magnetic stirring. The initial bacterial concentration was maintained at 107 CFU/ml and the tests were performed at room temperature for 120 min. At given time intervals, 1 ml suspension was collected and diluted appropriately by serial dilution in distilled water. To count the bacterial concentration, ready-to-use petrifilm (3M Petrifilm, USA) and prepared agar plates were used. After incubation for 48 h, the number of bacteria was manually counted using a colony counter. Furthermore, the antibacterial activity of as-synthesized particles without UV light was measured by applying zone inhibition method on *E. coli*. Using a spread plate method, nutrient agar plates were incubated with 1 ml of bacterial suspension containing around 106 colony forming units (CFU)/ml. The photocatalysts were gently placed on the inoculated plates, and were then incubated at 37 °C for 24 h. Zones of inhibition were determined by measuring the clear area formed around each photocatalyst.

3. Results and discussion

The representative FE-SEM images of different photocatalysts are shown in Fig. 1. It shows that the pristine ZnO flowers are micro sized and their size is decreased upon addition of TiO_2 NPs and $AgNO_3$ solution in the hydrothermal system. The possible cause of decrease in flower size might be due to the decrease in concentration of ZnO precursor per unit volume in the hydrothermal solution. P25 NPs and $AgNO_3$ present in the same volume of solution could sufficiently decrease the concentration of ZnO precursor per unit volume. Presence of $AgNO_3$ and TiO_2 NPs in the hydrothermal system not only sufficiently decreased the size of zinc oxide flowers but also formed a composite of Ag NPs decorated binary semiconductor system ($Ag/TiO_2/ZnO$) (Fig. 1d). Transmission electron microscope analysis (TEM) can be used to examine the morphology as well as composite structure of as-synthesized photocatalysts. The TEM images (Fig. 2a and b) reveal a unique flower-shaped morphology of ZnO particles, and Ag and TiO_2 NPs are well decorated on the surface of flowers. Ag NPs were deposited on the petal of bear ZnO flowers as well as on TiO_2 NPs attached on ZnO petals. The formation of Ag deposited binary semiconductor composite was further supported by TEM–EDX, shown in Fig. 2c. Here, Ag, Ti, and Zn are found along the selected line and revealed the formation of composite in nano structure.

The formation of composite photocatalyst was confirmed by FT-IR spectra. Fig. 3 shows the FT-IR spectra of ZnO, TiO_2/ZnO, and $Ag/TiO_2/ZnO$ particles. The broad absorption peaks around 3400 cm^{-1} and 1155 cm^{-1} are attributed to O–H stretching vibration of H_2O in ZnO and composite particles [18] which may be caused by moister absorption. A sharp peak around 1600 cm^{-1} is attributed to H–O–H bending vibration, which is assigned to a small amount of H_2O in ZnO crystals [19]. The medium weak band at 882 cm^{-1} is assigned to the vibrational frequency due to the Zn–O lattice. The significant decrease in intensity as well as slightly shifting towards higher value of the peak at 882 cm^{-1} in composite TiO_2/ZnO particle with compared to pristine ZnO revealed that chemically bonded TiO_2/ZnO composite was formed. The intensity of peaks at 3400, 1600, and 892 cm^{-1} shifted towards lower value after loading Ag NPs on composite, indicated the formation of $Ag/TiO_2/ZnO$ composite particles. Moreover, the shifted peak of ZnO (at 882 cm^{-1}) towards higher value when TiO_2 was loaded to ZnO, was found to be significantly shifted towards lower value after Ag loading (Fig. 3) which revealed the deposition of Ag as well as formation of metal binary semiconductor composite. Ag atom is far heavier than Zn atom, therefore according to the well established theories of irrational modes in mixed crystals the substitution should result in a downward shift of the fundamental transverse optical phonon mode [20].

The crystalline structure of as-prepared pristine and composite ZnO photocatalysts with the corresponding 2θ values are presented in Fig. 4. All the diffraction peaks for ZnO can be indexed to wurtzite structure (JCPDS card no. 80-0075) for both pristine and composite samples which are similar to the authors previous report [3]. The presence of sharp peak at $2\theta = 24.9$ (crystal plane 101, for rutile phase of TiO_2) [9] in nanocomposite revealed that TiO_2 is well-doped on the surface of ZnO nano-flower (Fig. 4b).

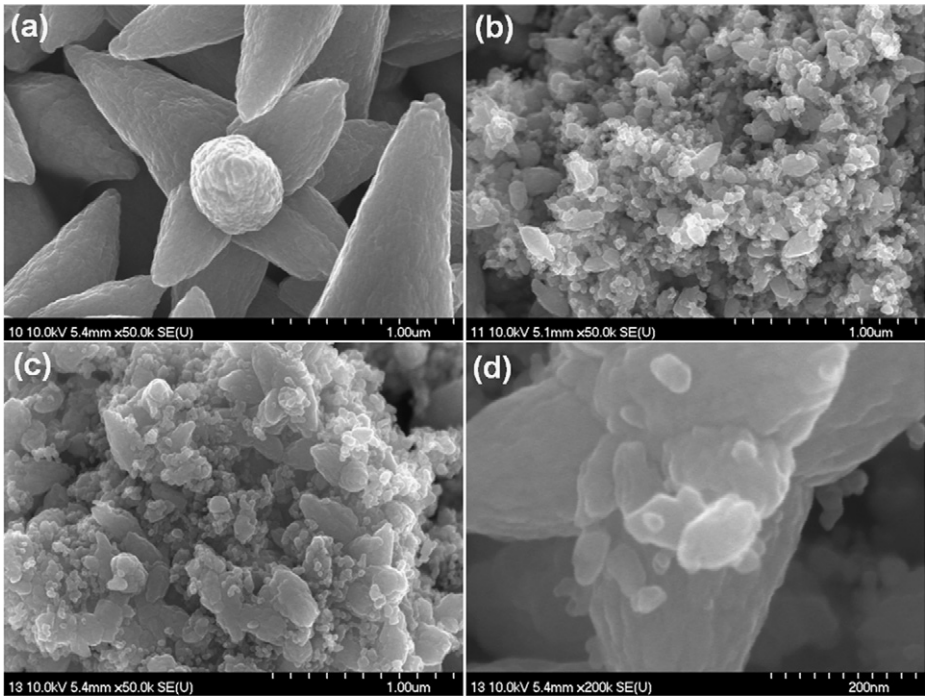

Fig. 1. FE-SEM images of (a) pristine ZnO, (b) TiO_2/ZnO, (c) $Ag/TiO_2/ZnO$ particles, and (d) high magnification of (c).

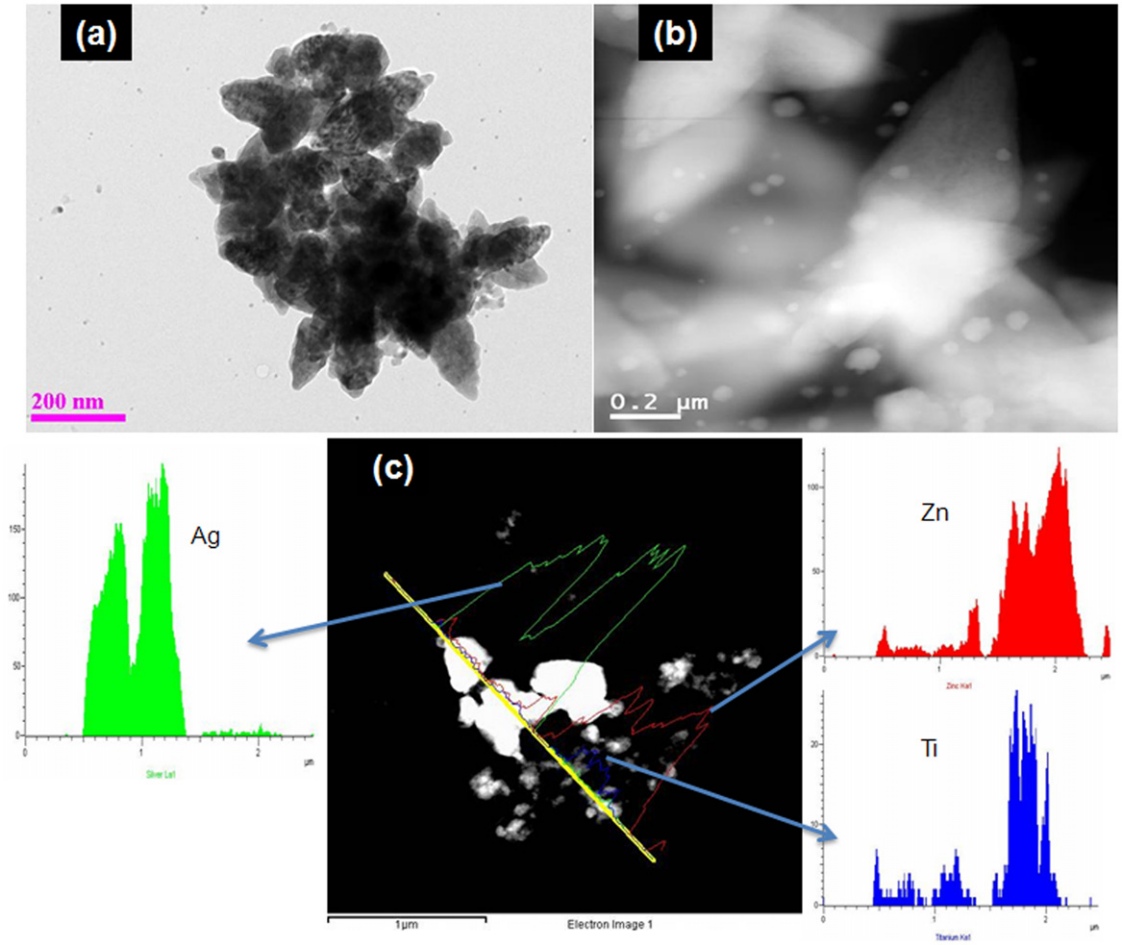

Fig. 2. (a and b) TEM images of $Ag/TiO_2/ZnO$ particles and (c) line EDX of $Ag/TiO_2/ZnO$ composite showing different metals.

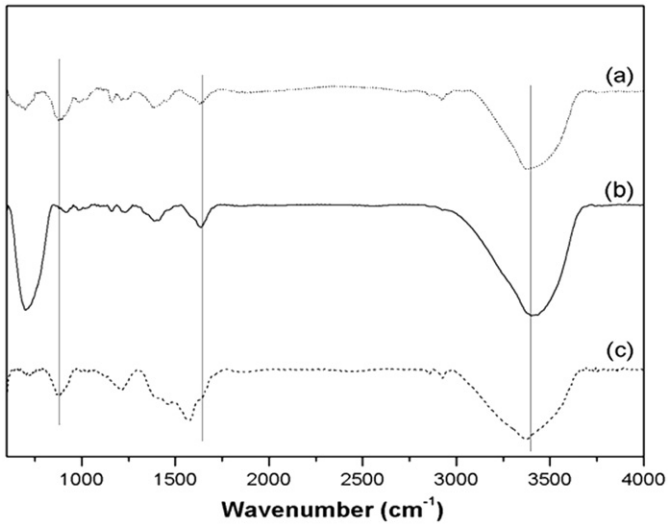

Fig. 3. FT-IR of (a) pristine ZnO, (b) TiO_2/ZnO, and (c) $Ag/TiO_2/ZnO$ particles.

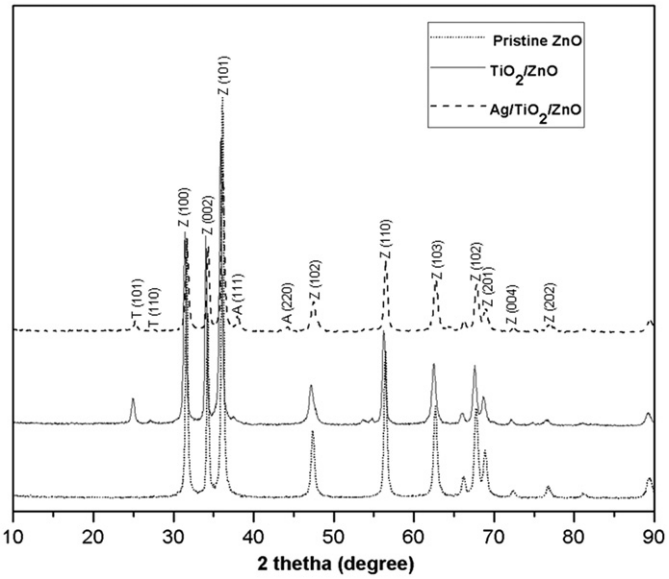

Fig. 4. XRD patterns of different photocatalysts.

The extra peaks on $Ag/TiO_2/ZnO$ composite particles compared to pristine ZnO and TiO_2/ZnO composite at 2θ values of 38, 44, and 64.3 corresponding to the crystal planes (111), (200), and (220), respectively, indicate the presence of Ag metal (JCPDS card no 04-0783) on binary semiconductor composite. The peak intensity of ZnO was

found to be decreased upon TiO_2 NPs deposition. Similarly, the intensity of TiO_2 in Ag doped composite photocatalyst was sufficiently decreased with compared to those of TiO_2/ZnO composite and revealed that Ag NPs were deposited not only on ZnO but also on TiO_2 NPs. Furthermore, the diffraction peaks of the ZnO in composite are shifted to small degree compared with the peaks of pristine ZnO which is the indication of formation of composite.

Photoluminescence (PL) spectra of as-synthesized photocatalysts were recorded at room condition and shown in Fig. 5. The spectra mainly consist of two emission bands. The first band is the UV near-band-edge (NBE) emission with a wavelength of ≈ 415 nm [21]. Sharp NBE emission peak is attributed to the recombination of photogenerated electrons and holes [22]. The decreased in intensity at 415 nm in composite particles indicates that the rate of recombination between photogenerated e–h might be lower, which is beneficial for photocatalytic process. The lowest intensity of this peak in Ag/TiO_2/ZnO is the indication of its highest photocatalytic efficiency. The PL spectrum also shows a peak around ≈ 531 nm which can be likely attributed interstitial oxygen [22,23]. The blue–green band around 482 nm was probably caused by radiative transition of electron from shallow donor levels, created by the oxygen vacancy to valence band [24].

The photocatalytic activity of the as-synthesized photocatalysts was evaluated by the degradation aqueous solution of reactive black 5 under mild UV irradiation (20% intensity). From Fig. 6, it is clear that the efficiency of ZnO flower is increased when composite is formed with Ag/TiO_2. This outcome may occur because of the unique properties of Ag NPs provided to TiO_2 and ZnO particles. Ag NPs deposited on the ZnO flowers or TiO_2 NPs attached with ZnO act as electron traps and enhance the e–h separation and the subsequent transfer of trapped electrons to the adsorbed O_2, which acts as an electron

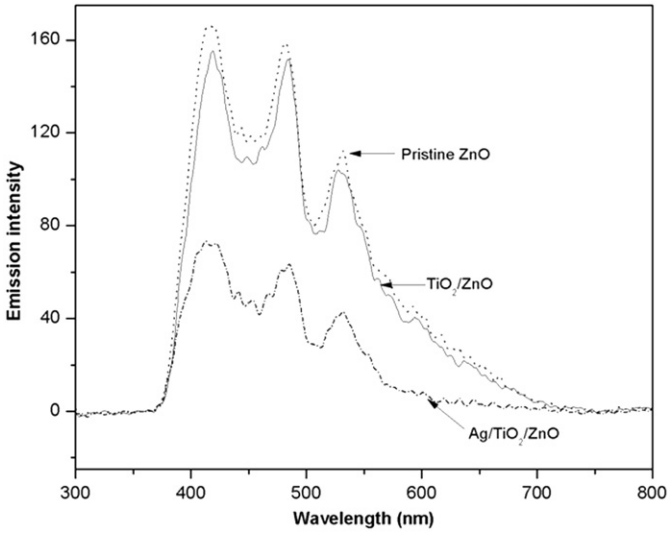

Fig. 5. PL spectra of different photocatalysts.

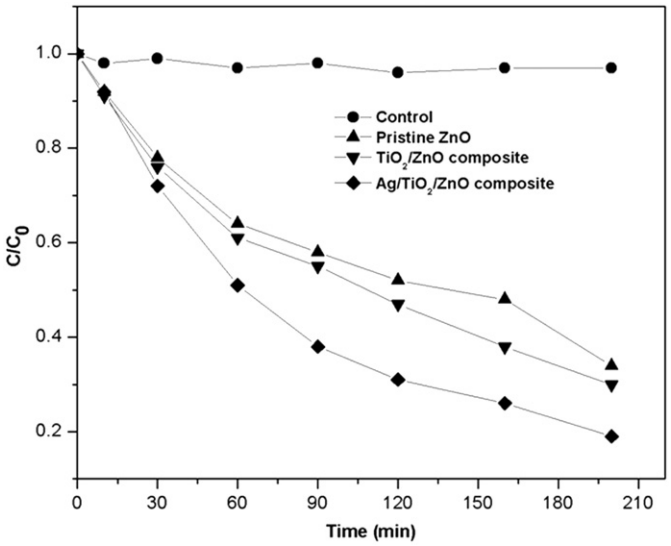

Fig. 6. Comparison of the reactive black 5 photodegradation using different photocatalysts.

acceptor. Furthermore, higher chemical activity of the Ag-loaded semiconductor particles can be explained by considering the formation of locally Schottky junctions with high potential gradients established by Schottky barrier than at the semiconductor/dye interface. Therefore, efficient charge separation of the light-generated e–h pairs can be achieved [25–27] which is also confirmed from decreased intensity of PL spectra described above. It may consider that in Ag/TiO_2/ZnO composite, the excited electrons of ZnO and TiO_2 can quickly transfer from the conduction band of ZnO or TiO_2 to Ag, and then effectively suppresses the recombination of photo-generated charge carriers, leaving more charge carriers to form highly reactive species (O_2, $\cdot OH$) and promote the degradation of dyes. It is further supported by our photoluminescence data (Fig. 5). The low intensity of the peak at 415 nm in composite with compared to the pristine ZnO indicates that the rate of recombination between photogenerated e–h might be lower, which is beneficial for photocatalytic process [28].

Economically and environmentally friendly photocatalyst should provide easiness of particles separation and their recovery from the reaction system after photocatalysis for practical application. For the separation ability test of photocatalysts, we performed sedimentation process of 3 h photodegraded solution (under UV light with continuous stirring) of composite Ag/TiO_2/ZnO photocatalyst. Similar to our previous report [3], Ag/TiO_2/ZnO composite after 30 min of sedimentation showed that this process was almost completed within this time. Therefore, one of the advantages of our as-synthesized photocatalytic particles is that they can be conveniently separated to recycle the catalyst. The efficiency of composite photocatalyst in recycle use was also evaluated in this work (Fig. 7). It was found that the efficacy of initially used and reused composite photocatalyst up to three cycles was

nearly similar for the degradation of reactive black 5. The slightly decreased in photocatalytic activity during cyclic use might be due to the accumulated organic intermediates on the surface of the catalyst which could affect the adsorption of dyes.

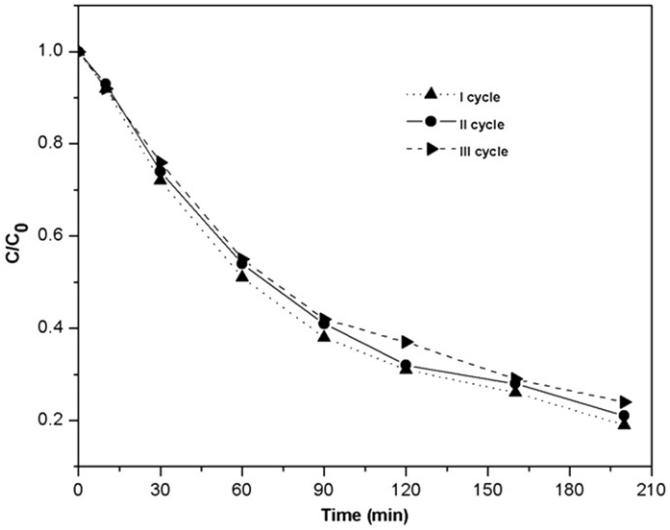

Fig. 7. Reusability of $Ag/TiO_2/ZnO$ composite up to three cycles.

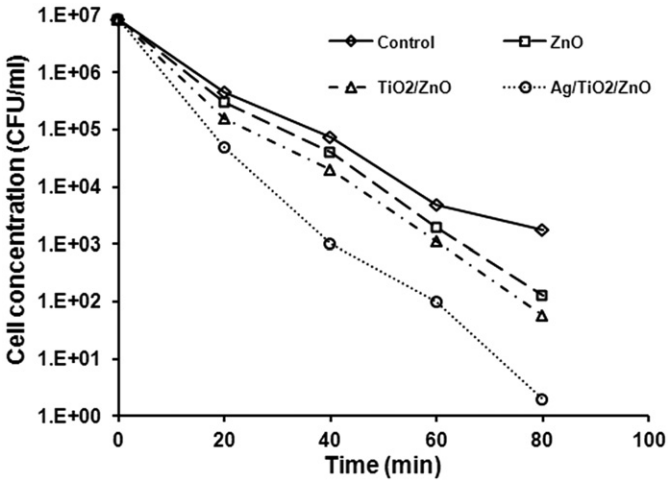

Fig. 8. Antibacterial efficiency of different photocatalysts on gram-negative *E. coli* bacteria under mild UV radiation.

The goal of this work is not only to make antibacterial material even in the absence of UV light but also decorate binary semiconductor particles with Ag NPs at the time of hydrothermal growth (one pot synthesis) because most of the reported works have used one extra process (photochemical deposition of Ag from $AgNO_3$ solution) for the same propose. The effect of one pot Ag loaded binary semiconductor composite on the antibacterial efficiency was measured using mild UV irradiation of bacterial solution at room temperature. The antibacterial capacity without UV light was also evaluated by zone inhibition method. Fig. 8 shows the antibacterial effect of as-prepared photocatalyst under mild (20% intensity) UV radiation. It shows that $Ag/TiO_2/ZnO$ has the best antimicrobial effect among the synthesized catalysts. The cause of the highest antibacterial capacity of $Ag/TiO_2/ZnO$ under UV radiation is same as explained in dye degradation. However, far better activity of $Ag/TiO_2/ZnO$ (compared to TiO_2/ZnO) (Fig. 9) without UV radiation is attributed to the presence of Ag NPs on the surface of composite particles. The actual mechanism of killing microorganisms with Ag in absence of UV light is not clear. Some researchers have proposed that Ag has innate antibacterial activity [29]. It is reported that Ag^+ hinders DNA replication and inhibits the expression of ribosomal proteins and enzymes for ATP hydrolysis [30]. It is believed that Ag NPs display the same mechanism as Ag^+ and create a redox imbalance, which causes extensive bacterial death. Furthermore, the antibacterial activity of Ag NPs on the surface of the composite may be due to the plasmon resonance of the Ag NPs. Here, photoexcited electrons may transfer from the surface of Ag NPs to the conduction band of semiconductors. On the surface of the TiO_2 or ZnO NPs, the injected electrons from Ag NPs are trapped by O_2 molecules and the active species such as O_2, •OOH, •OH can be generated for the bacterial destruction [31,32]. The larger diameter of inhibition zone (DIZ) in $Ag/TiO_2/ZnO$ with compared to the DIZ of TiO_2/ZnO (Fig. 9) clearly revealed the effect of Ag NPs on antibacterial properties of composite particles.

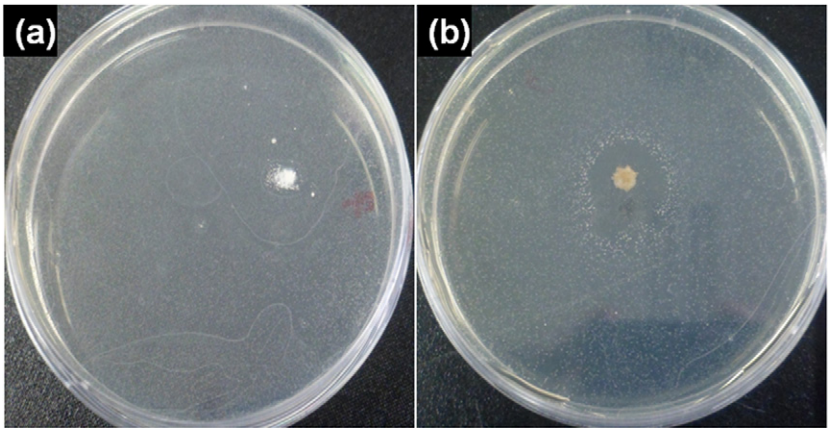

Fig. 9. Zones of inhibition tests for (a) TiO_2/ZnO and (b) $Ag/TiO_2/ZnO$ composites towards gram-negative *E. coli* bacteria.

4. Conclusions

In this work, flower-shaped ZnO particles hierarchically assembled with TiO_2 and Ag NPs were prepared by facile one-pot hydrothermal process. The $Ag/TiO_2/ZnO$ composite displayed excellent photocatalytic performance which is attributed to a good electron acceptor favoring the transfer of photo-generated electrons from the conduction band of ZnO or TiO_2 to Ag NPs. As-synthesized composite particles have also good antibacterial property. Furthermore, the photocatalytic particles attached on the big size ZnO flower can be easily recovered from reaction system after reaction which makes it an economically and environmentally friendly photocatalyst.

Acknowledgments

One of the authors Hem Raj Pant kindly acknowledges the financial support from the research fund of Chonbuk National University Grant Fellow Project 2012 (Research Associate Program) as well a grant from the Korean Ministry of Education, Science and Technology (MIST) through the National Research Foundation (NRF) (Project no. 2012-0113423). We would also like to thank Mr. Lee Young-Boo, KBSI, Jeonju branch for TEM analysis.

References

[1] A.D Paola, E. Garcia-Lopez, G. Marci, L. Palmisano, A survey of photocatalytic materials for environmental remediation, Journal of Hazardous Materials 211–212 (2012) 3–29.
[2] K.R. Raghupathi, R.T. Koodali, A.C. Manna, Size-dependent bacterial growth inhibition and mechanism of antibacterial activity of zinc oxide nanoparticles, Langmuir 27 (2011) 4020–4028.
[3] H.R. Pant, C.H. Park, B. Pant, L.D. Tijing, H.Y. Kim, C.S. Kim, Synthesis, characterization, and photocatalytic properties of ZnO nano-flower containing TiO_2 NPs, Ceramics International 38 (2012) 2943–2950.
[4] L.E. Greene, M. Law, J. Goldberger, F. Kim, J.C. Johnson, Y.F. Zhang, R.J. Saykally, P.D. Yang, Low-temperature wafer-scale production of ZnO nanowire arrays, Angewandte Chemie, International Edition 42 (2003) 3031–3034.
[5] S. Music, D. Dragcevic, S. Popovic, Influence of synthesis route on the formation of ZnO particles and their morphology, Journal of Alloys and Compounds 429 (2007) 242–249.
[6] F.A. Sheikh, M.A. Kanjwal, H.Y. Kim, H. Kim, Fabrication of titanium dioxide nanofibers containing hydroxyapatite nanoparticles, Applied Surface Science 275 (2010) 296–301.
[7] J. Zhao, Y. yang, Photocatalytic oxidation for indoor air purification: a literature review, Building and Environment 38 (2003) 645–654.
[8] L. Reijenders, Hazard reduction for the application of titania nanoparticles in environmental technology, Journal of Hazardous Materials 152 (2008) 440–445.
[9] H.R. Pant, M.P. Bajgai, K.T. Nam, Y.A. Seo, D.R. Pandeya, S.T. Hong, H.Y. Kim, Electrospun nylon-6 spider-net like nanofibers mat containing TiO_2 nanoparticles: a multifunctional nanocomposite textile material, Journal of Hazardous Materials 185 (2011) 124–130.
[10] M. Jakob, H. Levanon, P.V. Kamat, Charge distribution between UV-irradiated TiO_2 and gold nanoparticles. Determination of shift in Fermi level, Nano Letters 3 (2003) 353–358.
[11] L. Shang, B. Li, W. Dong, B. Chen, C. Li, W. Tang, G. Wang, J. Wu, Y. Ying, Heteronanostructure of Ag particle on titanate nanowire membrane with enhanced photocatalytic properties and bactericidal activities, Journal of Hazardous Materials 178 (2010) 1109–1114.
[12] B. Cheng, Y. Le, J. Yu, Preparation and enhanced photocatalytic activity of $Ag@TiO_2$ core–shell, Journal of Hazardous Materials 177 (2010) 971–977.
[13] T. Matsunaga, R. Tomoda, T. Nakajima, H. Wake, Photo electrochemical sterilization of microbial cells by semi-conductor powders, FEMS Microbiology Letters 29 (1985) 211–214.
[14] J. Keleher, J. Bashant, N. Heldt, L. Johnson, Y. Li, Photo-catalytic preparation of silver-coated TiO_2 particles for antibacterial applications, World Journal of Microbiology and Biotechnology 18 (2002) 133–139.
[15] K. Page, R.G. Palgrave, I.P. Parkin, M. Wilson, S.L.P. Savin, A.V. Chadwick, Titania and silver–titania composite films on glass-potent antimicrobial coatings, Journal of Materials Chemistry 17 (2007) 95–104.
[16] X.Z. Li, F.B. Li, Study of Au/Au^{3+}–TiO_2 photocatalysts toward visible photooxidation for water and wastewater treatment, Environmental Science and Technology 35 (2001) 2381–2387.
[17] H. Frenzel, A. Lajn, M. Brandt, H. von Wenckstern, G. Biehne, H. Hochmuth, M. Lorenz, M. Grundmann, ZnO metal-semiconductor field-effect transistors with Ag-Schottky gates, Applied Physics Letters 92 (2008) 192108.
[18] K. Nakamoto, Infrared and Raman Spectra of Inorganic and Coordination Compounds, Parts – A and B, John Wiley & Sons, New York, 1997.
[19] A. Jagannatha Reddy, M.K. Kokila, H. Nagabhushan, R.P.S. Chakradhar, C. Shivakumar, J.L. Rao, B.M. Nagabhushan, Structural, optical and EPR studies on ZnO:Cu nanopowders prepared via low temperature solution combustion synthesis, Journal of Alloys and Compounds 509 (2011) 5349–5355.
[20] D.W Taylor, Optical Properties of Mixed Crystals, North-Holland, 1988, pp. 35–131 (Chapter 2).
[21] J. Lim, K. Shin, H.W. Kim, C. Lee, Effect of annealing on the photoluminescence characteristics of ZnO thin films grown on the sapphire substrate by atomic layer epitaxy, Materials Science and Engineering B 107 (2004) 301–304.
[22] J. Yang, J. Zheng, H. Zhai, X. Yang, L. Yang, Y. Liu, J. Lang, M. Gao, Orented growth of ZnO nanostructures on different substrates via hydrothermal method, Journal of Alloys and Compounds 489 (2010) 51–55.
[23] J.H. Yang, J.H. Zheng, H.J. Zhai, L.L. Yang, Low temperature hydrothermal growth and optical properties of ZnO nanorods, Crystal Research and Technology 44 (2009) 87–91.
[24] D. Chu, Y. Zeng, D. Jiang, Hydrothermal synthesis and optical properties of Pb^{2+} doped ZnO nanorods, Materials Letters 60 (2006) 2783–2785.
[25] C.Y. Wang, C.Y. Liu, X. Zheng, J. Chen, T. Shen, Effect of platinum on the photocatalytic decomposition of 2-chlorophenol in aqueous solution by UV/TiO_2, Colloids and Surfaces A 131 (1998) 271–280.
[26] V. Subramanian, E. Wolf, P. Kamat, To what extent metal nanoparticles (Au, Pt, Ir) improve the photocatalytic activity of TiO_2 films, Journal of Physical Chemistry B 105 (2001) 11439–11446.
[27] W.S. Kuo, P.H. Ho, Solar photocatalytic decolorization of methylene blue in water, Chemosphere 45 (2001) 77–83.
[28] J. Yang, J. Zheng, H. Zhai, X. Yang, L. Yang, Y. Liu, J. Lang, M. Gao, Orented growth of ZnO nanostructures on different substrates via hydrothermal method, Journal of Alloys and Compounds 489 (2010) 51–55.
[29] V. Rupa, D. Manikandan, D. Divakar, T. Sivakumar, Effect of deposition of Ag on TiO_2 nanoparticles on the photodegradation of Reactive yellow-17, Journal of Hazardous Materials 147 (2007) 906–913.
[30] M. Yamanaka, K. Hara, J. Kudo, Bactericidal actions of a silver Ion solution on *Escherichia coli*, studied by energy-filtering transmission

electron microscopy and proteomic analysis, Applied and Environmental Microbiology 71 (2005) 7589–7593.

[31] H.M. Sung-Suh, J.R. Choi, H.J. Hah, S.M. Koo, Y.C. Bae, Comparison of Ah deposition effect on the photocatalytic activity of nanoparticulate TiO_2 under visible and UV light irradiation, Journal of Photochemistry and Photobiology A 163 (2004) 37–44.

[32] H.R. Pant, D.R. Pandeya, Ki Taek Nam, Woo-il Baek, Seong Tshool Hong, Hak Yong Kim, Photocatalytic and antibacterial properties of a TiO_2/nylon-6 electrospun nanocomposite mat containing silver nanoparticles, Journal of Hazardous Materials 189 (2011) 465–471.